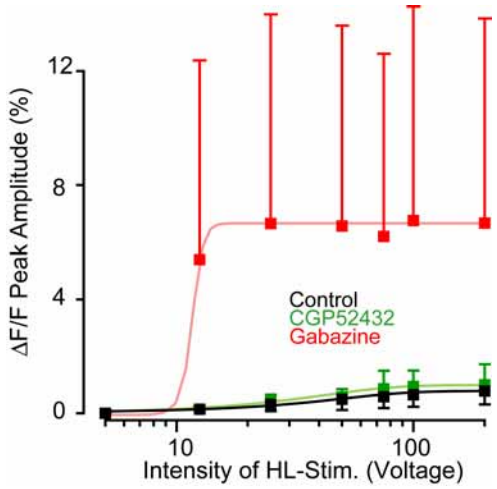


**Supplementary Figure 1.** Non-normalized data of *ΔF*/*F* peak amplitude of dendritic $Ca^{2+}$ signals evoked by hind limb stimulation.CGP52432 (green, $n = 6$) and gabazine (red, $n = 6$) were applied to cortical surface (see text).

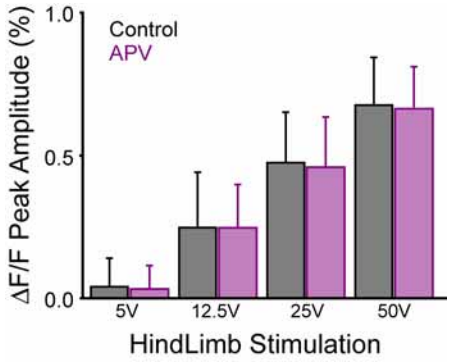


**Supplementary Figure 2.** Hindlimb stimulation evoked *ΔF*/*F* peak amplitude of dendritic $Ca^{2+}$ signals ($n = 6$) before and after application of APV (100 μM), an antagonist of NMDA receptors, to cortical surface. $P > 0.1$.

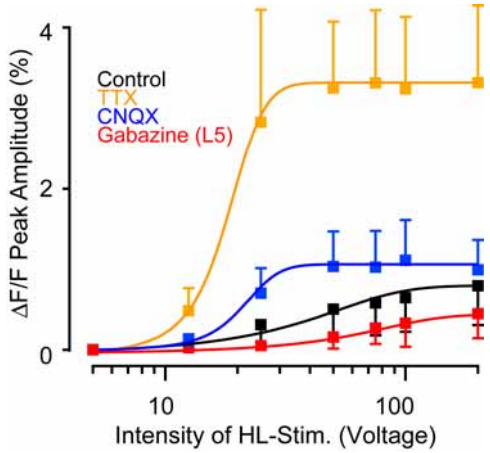


**Supplementary Figure 3.** Non-normalized data of *ΔF/F* peak amplitude of dendritic $Ca^{2+}$ signals with TTX (orange, $n = 5$), CNQX (blue, $n = 5$) and gabazine (red, $n = 5$). The drugs were applied into L5 separately (see text).

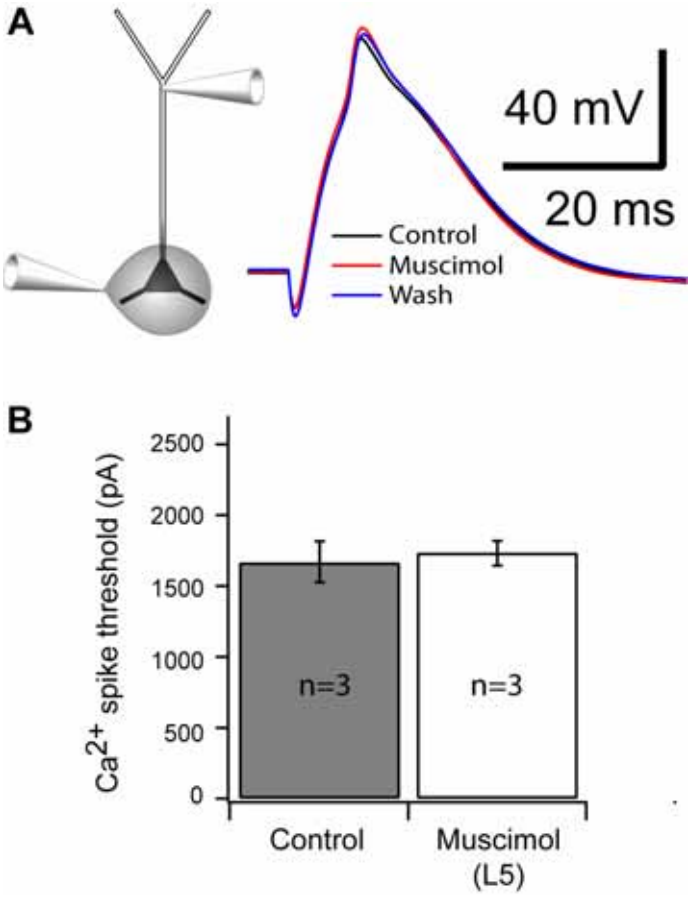


**Supplementary Figure 4.** Inhibition of $Na^+$ and activation of $GABA_A$ receptor channels at the peri-somatic area, does not influence the generation of dendritic $Ca^{2+}$ spikes. **a,** Left, Schematic diagram of experiment. A dendritic patch recording at >500 µm from the cell body was used to generate and record a $Ca^{2+}$ spike. TTX (3 µM) was local applied to the peri-somatic region. Right, Dendritically recorded traces showing that suprathreshold $Ca^{2+}$ spikes (red) could be generated with current injection above 2300 pA in an all-or-none fashion. **b**, Muscimol did not change the threshold for the generation of dendritic $Ca^{2+}$ spikes with dendritic current injection ($n = 3$; $P = 0.42$). Local application

of muscimol (20 μM) to L5 (analogous to the in vivo experiments of Fig. 2) did not change the threshold for dendritic $Ca^{2+}$ spikes using dendritic current injection (1.67 ± 0.25 nA vs. 1.73 ± 0.15 nA, $P$ = 0.42, $n$ = 3, data not shown), indicating that somatic inhibition has very little effect on the generation of dendritic $Ca^{2+}$ spikes.

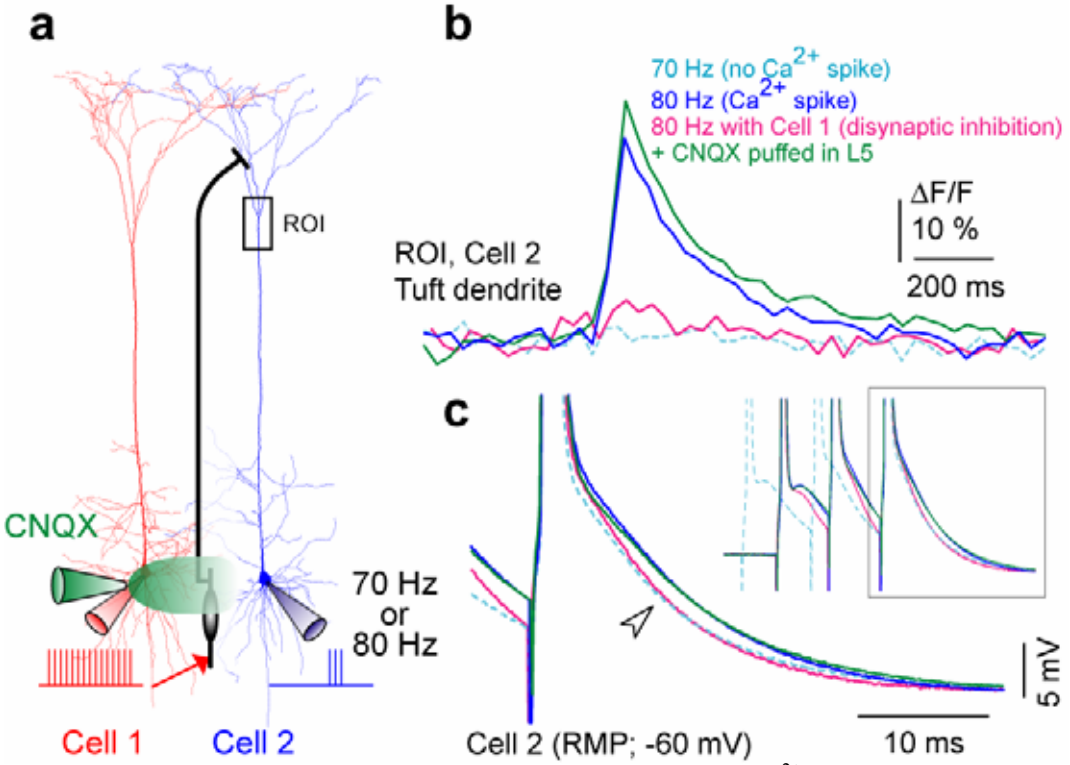


**Supplementary Figure. 5.** Disynaptic inhibition blocks dendritic $Ca^{2+}$ activity induced by high-frequency back-propagating APs. **a,** Experimental diagram showing reconstructed L5 pyramidal neurons and recording sites (same experiment as in Fig. 3 e & f). **b**, We have previously shown that there is a critical frequency of back-propagating APs which generate dendritic $Ca^{2+}$ spikes[23]. Here, trains of somatic action potentials at a sub-critical frequency (70 Hz) did not evoke a dendritic calcium transient in the apical tuft initiation zone (dashed cyan), whereas an increase of 10 Hz in the frequency of back-propagating APs (the critical frequency, 80 Hz) evoked substantial, all-or-none $Ca^{2+}$ transient in the same region (dark blue) with a accompanying increase in somatic membrane potential directly after the last AP in the train (see part c). Simultaneous disynaptic inhibition abolished the dendritic transient (pink) which was recovered after application of 20 μM CNQX to L5 (green). **c**, The after-depolarizing potential (ADP) measured after the last AP at the soma reflects the changes in $Ca^{2+}$ influx into the dendritic $Ca^{2+}$ spike initiation zone. Magnified view of the ADPs (arrowhead). An increase in the amplitude of the ADP from 70 to 80 Hz was indicative of a dendritic $Ca^{2+}$ spike. Disynaptic inhibition reversed the amplitude of the ADPs to sub-critical frequency values (pink; $P < 0.05$, $n = 8$). The amplitude of the ADPs recovered after perisomatic application of CNQX to control values (green).

# Supplementary model description

## *Remarks on the model design*

We present a mathematical model which allows us to describe the various pharmacological blocking experiments and to reproduce the corresponding population calcium responses as presented in the main text. A minimal phenomenological model which captures the dependence of the calcium response function from the feedforward and feedback connection strengths consists of a simple feedback circuitry as shown in the Supp. Fig. M3. This simple feedback circuitry is mathematically deduced from the full model (Supp. Figs M1, 2) and describes the calcium signal *C* in response to a stimulus of strength *S*.

In the steady state the calcium response function *C(S)* is a sigmoidal which depends on three effective parameters, the saturation level, the half-activation (`shift´), and the gain. Each of these parameters can be expressed in terms of the feedforward/feedback connection strengths and the calcium spike characteristics (see Eqs 14 – 15). This minimal model captures the differential effects of the feedforward and feedback inhibition on the gain and the shift of the response function (Fig. 4d, main text and Full Methods).

The simple feedback circuitry also allows us to fit the response curves for the various pharmacological blocking experiments. In fact, since each of the five response curves can be characterized by 3 parameters (saturation, shift and gain) it is always possible to fit each by adapting the 3 model parameters, the number of recruitable pyramidal neurons (determining the saturation level), the strength of the feedforward connection (affecting the shift), and the strength of the feedback connection (affecting gain and shift). To reduce the number of free parameters we further constrain the model by considering pyramidal neurons embedded in a microcircuitry with distributed excitatory and inhibitory feedback and feedforward projections. For each pharmacological blocking experiment we then define a set of connections which are deleted from the model microcircuitry to determine the corresponding calcium response curve (see Supp. Fig. M4). Given these sets we tuned 10 parameters values (6 connections strengths and 4 different numbers of recruitable pyramidal neurons) to fit the 5 sigmoidal response curves which by themselves would require a total of 15 values (see Table 1). Hence, the structure of the model circuitry allows us to reduce the 15 degrees of freedom to effectively 10 free parameter choices. The extended model is therefore constrained enough to unravel intrinsic dependencies in the data and to explain them with a reduced set of physiologically interpretable (although not yet measured) parameters.

A second step beyond the simple calcium feedback circuitry consists in introducing a 2-compartment pyramidal cell model with current-to-frequency transfer function extracted from previous data (Larkum et al., 2004). All the parameter values describing the pyramidal neurons are fixed to the values extracted from this previous data. Including these model pyramidal cells represents a genuine extension since it takes the current-frequency feedback circuitry into account which underlies the recruitment of dendritic calcium currents. As a consequence, for instance, the effective feedforward drive of the calcium signal becomes itself dependent on the feedback connection strength. In fact, the feedback contributes to the dendritic current already before it is crossing the calcium spike threshold. Beside these complications, we also consider the voltage interactions between the somatic and dendritic compartments.

The mathematical analysis of the extended model yields a reduction of the full microcircuitry of pyramidal cells and interneurons to the original simple calcium feedback circuitry, but now with parameters being expressed in terms of biophysical quantities (Eqs 15&16). It provides an explicit dependence of the population calcium response curves on each of the pyramidal cell and microcircuitry parameters. The close link between phenomenological observations and the

microscopic parameters allows us to make quantitative predictions for further pharmacological modulations, e.g. of specific connections to or from Martinotti cells (see Supp. Fig. M5).

## *The model*

**Pyramidal neurons and microcircuitry.** We consider a population of $N$ pyramidal neurons, each with a somatic and dendritic compartment (Fig. M1, M2). The somatic compartments receive a feedforward synaptic current of the form

$$I_{syn}^{som}(S) = \alpha^{ffsom} \log S \qquad (1)$$

in response to a sensory stimulation of strength $S$. The factor is composed of an excitatory component and an inhibitory component mediated through an inhibitory neuron $\alpha^{ffsom} = \alpha_{ex}^{ffsom} - \alpha_{inh}^{ffsom}$ .The logarithmic dependence on the stimulus strength represents Weber's law and arises from the various saturation mechanisms in the upstream sensory processing. These input currents are assumed to last for a duration of at least 90ms following the electrical hind limb pulse as this time delay corresponds to the observed delay of the calcium fluorescence peak activity.

The total synaptic input to the dendritic compartment, $I_{syn}^{den}(S)$, is composed of feedback input from the pyramidal cell population itself and the feedforward input, both targeting the dendrite either directly or through the Martinotti cells (Fig. M2). To simplify matters we assume that the transfer functions of the Martinotti cells and the second inhibitory neuron in L5 are linear. The total synaptic input targeting the dendritic compartment can be written in the form

$$I_{syn}^{den} = \frac{\alpha^{fbden}}{N} \sum_{i=1}^{N} f_i^{pyr}(S) + \alpha^{ffden} \log S \,. \qquad (2)$$

where $f_i^{pyr}(S)$ represents the firing rate of the $i$ th pyramidal neuron and the constants are $\alpha^{fbden} = \alpha_{ex}^{fbden} - \alpha_{inh}^{fbden}$ and $\alpha^{ffden} = \alpha_{ex}^{ffden} - \alpha_{inh}^{fbden}\left(\alpha_{ex}^{ffM} - \alpha_{inh}^{ffM}\right)$, see Fig. M2. Note that the total feedforward input current to the Martinotti cells is $I^{ffM}(S) = \left(\alpha_{ex}^{ffM} - \alpha_{inh}^{ffM}\right)\log S$, and that the (inhibitory) feedforward input to the dendrites mediated by the Martinotti cells is $-\alpha_{inh}^{fbden} I^{ffM}(S)$. In turn, the (inhibitory) feedback component from the pyramidal neurons mediated by the same Martinotti cells is $-\alpha_{inh}^{fbden} 1/N \sum f_i^{pyr}(S)$. Adding to this the excitatory feedforward and feedback inputs yields Eq. 2.

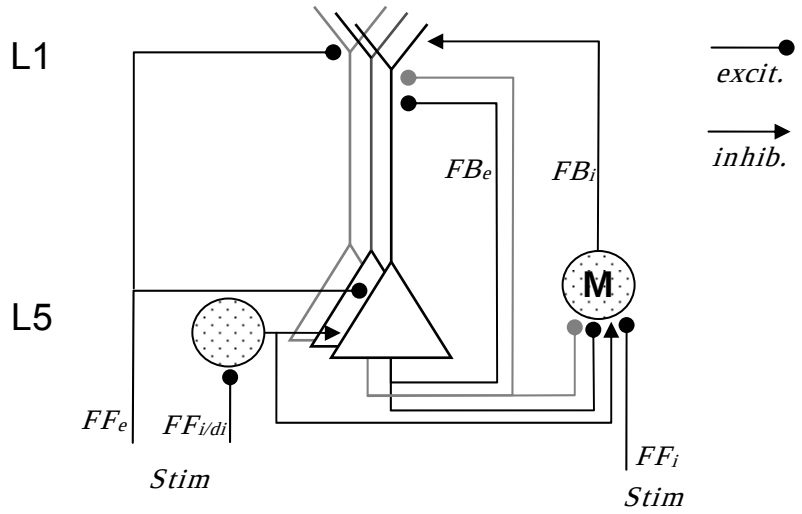


**Supplementary Figure M1.** *Model of the cortical microcircuitry. A population of layer 5 pyramidal neurons driven by the stimulus (Stim) through excitatory feedforward connections ($FF_e$) to both the somatic and dendritic region, and by inhibitory feedforward connections ($FF_i$) via Martinotti cells (*M*) to the dendritic region. Feedback from the pyramidal neurons is directly exciting the pyramidal cell dendrites ($FB_e$), or is inhibiting them via Martinotti cells ($FB_i$). The soma also receives direct inhibition, while the dendrites are disinhibited via inhibition targeting Martinotti cells ($FF_{i/di}$). Feedforward and feedback input to the dendrites differently affect the population calcium response.*

**Passive pyramidal cell properties.** The 2-compartment pyramidal cell model is specified by the somatic and dendritic membrane resistance $R_m^{som}$ and $R_m^{den}$, respectively, and transfer resistance $R_T$ (Fig. M2). Given the 90ms delay of the peak fluorescence signal with respect to the sensory stimulation, we assume that the somatic and dendritic voltages converged to a steady state. The total synaptically generated current in the dendrite (i.e. the synaptic currents from soma and dendrite without dendritic calcium current) then becomes

$$I_0^{den}(S) = \lambda^{som} I_{syn}^{som} + (1-\lambda^{den}) I_{syn}^{den} \quad , \qquad (3)$$

where $\lambda^{som} = R_m^{som} / (R_m^{som} + R_m^{den} + R_T)$ and $\lambda^{den} = R_m^{den} / (R_m^{som} + R_m^{den} + R_T)$ represent the fractions of currents leaking away from the soma and dendrite, respectively, into the other compartment (for a derivation of Eq. 3 see Endnote 1). Hence, the dendritic compartment shares a fraction $\lambda^{som}$ of the somatic input, and a fraction $(1-\lambda^{den})$ of the dendritic input.

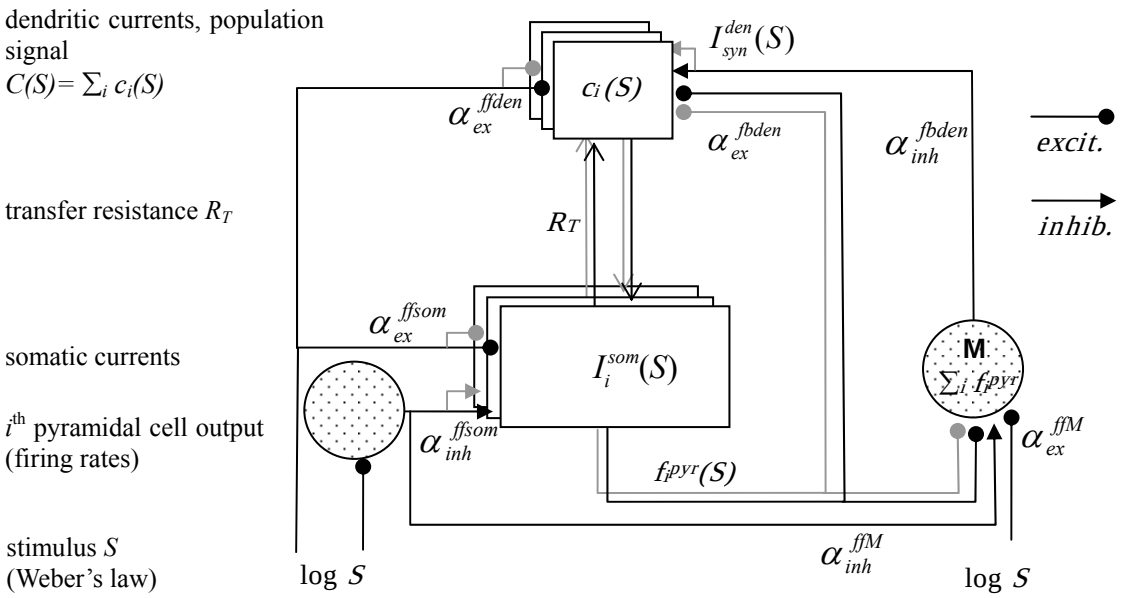


**Supplementary Figure M2.** *Model and mathematical quantities. A population of layer 5 pyramidal neurons, each with a somatic compartment receiving feedforward input, and a dendritic compartment receiving feedforward and feedback input via excitatory and inhibitory (Martinotti) neuron. If the total input to the dendrite, $I_0^{den}(S)$, in response to stimulus S exceeds a cell-specific threshold ($\theta_i$), a calcium spike of strength c is elicited. The measured calcium fluorescence signal corresponds to the population calcium signal $C(S)= \sum_I c_i(S)$ summed across the dendrites of all pyramidal neurons i=1,..,N.*

**Dendritic calcium spikes.** Whenever the total synaptically generated dendritic current $I_0^{den}(S)$ exceeds a cell specific threshold $\theta_i$ (with $i=1,...,N$) a dendritic calcium spike is triggered. This spike is modeled as a plateau current of constant strength $c$[1]. The dendritic calcium current in pyramidal cell $i$ is captured by the Heaviside step function

$$c_i(S) = c\,\mathrm{H}\left(I_0^{den}(S) - \theta_i\right) = \begin{cases} c & \text{if } I_0^{den}(S) > \theta_i \\ 0 & \text{else} \end{cases}, \qquad (4)$$

where H($x$ = 0 if $x$<0 and 1 else. We assume that the calcium thresholds $\theta_i$ of the $i$ pyramidal neurons are distributed (Gaussian-like) around some mean $\theta_0$ with standard deviation σ.
The population calcium signal in response to stimulus $S$ is

$$C(S) = \sum_{i=1}^{N} c_i(S)\ , \qquad (5)$$

and this corresponds to the quantity which is experimentally measured via calcium fluorescence.

**Pyramidal cell firing rate.** The dendritically generated current $I_{syn}^{den}(S) + c_i(S)$ electrotonically propagates to the soma where it adds up with the synaptic current $I^{ff}(S)$ targeting the soma. The total steady state current in the soma generated by the different synaptic inputs and the dendritic calcium

[1] Note: the data cannot distinguish between this and the case that dendritic spikes give variable amplitudes. In the 2nd case, the value $c$ can be interpreted as the average Ca2+ entry accompanying a dendritic spike.

spike is calculated to be

$$I_i^{som}(S) = \lambda^{den}\left(I_{syn}^{den}(S) + c_i(S)\right) + (1-\lambda^{som})\, I_{syn}^{som}(S)\,.^{\mathrm{i}} \qquad (6)$$

Next we assume that the somatic currents are transformed into asynchronous output firing rates of the pyramidal neurons according to the threshold linear transfer function

$$f_i^{pyr}(S) = g\,[I_i^{som}(S) - \Theta]^+\,, \qquad (7)$$

where $g>0$ is the gain of the *f-I* curve, $\Theta$ is the current threshold for generating somatic action potentials, and $[x]^+ = x$ if $x>0$ and $0$ else.

## *Model analysis*

To calculate the population calcium signal $C(S)$ we assume that the stimulation strengths is strong enough to fire the pyramidal neurons by the feedforward input alone. As a consequence, the somatic currents are always in the linear regime of the current-to-frequency transfer function. In this case the feedback circuitry presented in Fig. M2 can be explicitly solved for $C(S)$.

**Distribution of dendritic calcium spike thresholds.** To calculate $C(S)$ we further consider a continuous distribution of the dendritic calcium spike thresholds $\theta=\theta_i$. We consider a bell-shaped normalized threshold density $\rho\theta$ with mean $\theta$ and exponential decay on both sides according to

$$\rho(\theta) = \frac{1}{\sigma}\cdot\frac{1}{1+e^{(\theta-\theta_0)/\sigma}}\cdot\frac{1}{1+e^{-(\theta-\theta_0)/\sigma}}\,, \qquad (8)$$

where σ is the width of the exponential decay (Suppl. Fig. M5b, green curve). A Gaussian threshold distribution instead of distribution (8) would lead to qualitatively similar results but the density (8) is mathematically convenient (as it is the derivative of a Boltzmann function). Instead of the index $i$, the pyramidal neurons are now parameterized by their characterizing calcium threshold $\theta$. The dendritic calcium signal of pyramidal cell $\theta$ is then

$$c_\theta(S) = c\;\mathrm{H}(I_0^{den}(S) - \theta \qquad (4')$$

instead of (4).

**The population calcium signal.** To simplify the mathematical treatment we replace the sum defining the population signal (Eq. 5) by an integral across calcium responses parameterized by the calcium threshold. Assuming a density $\rho\theta$ of calcium thresholds, the dendritic calcium signal of the whole population becomes,

$$C(S) = N\int_{-\infty}^{\infty}\rho(\theta)\cdot c_\theta(S)\;d\theta = N\int_{-\infty}^{\infty}\rho(\theta)\cdot c\cdot\mathrm{H}(I_0^{den}(S)-\theta)\;d\theta = \frac{Nc}{1+e^{-(I_0^{den}(S)-\theta_0)/\sigma}}\,. \qquad (9)$$

For the calculation of this integral we refer to Endnote 2. Hence, the population response of the binary calcium spikes is a sigmoidal function in $I_0^{den}(S)$, with a gain $1/\sigma$ being the inverse width of the calcium threshold distribution $\rho\theta$: the wider the threshold distribution, the shallower the population response function. For strong stimulations, $I_0^{den}(S)$ becomes large and each neuron of the population elicits a dendritic calcium spike, yielding the maximal response $C(S)= Nc$.

**Deducing the calcium recurrence relation.** The formula for the population calcium signal $C(S)$ implicitly represents a recurrence relation as $C(S)$ also determines the dendritic current $I_0^{den}(S)$ occurring in (9). To address this recurrence relation we rewrite the synaptic current in the dendrite, Eq. 2, as

$$I_{syn}^{den}(S) = \alpha^{fbden}\int_{-\infty}^{\infty}\rho(\theta)\,f_\theta^{pyr}(S)\;d\theta + \alpha^{ffden}\log S\,, \qquad (10)$$

where we again replaced the index $i$ by $\theta$, and the normalized sum $1/N\,\Sigma_i f_i^{pyr}$ by the integral of $f_\theta^{pyr}$, weighted by the normalized threshold density $\rho(\theta)$.

Next we use the assumption that the sensory stimulations always drive the pyramidal neurons. We can then write the pyramidal cell firing rates (7) in the form

$$f_\theta^{pyr} = g\left(\lambda^{den}(I_{syn}^{den} + c_\theta) + (1-\lambda^{som})I_{syn}^{som} - \Theta\right), \quad (11)$$

where we substituted the somatic current $I_\theta^{som} = \lambda^{den}(I_{syn}^{den} + c_\theta) + (1-\lambda^{som})I_{syn}^{som}$ given by Eq. 6 and where we dropped the dependency on *S*. Plugging this into the above integral (10), and calculating the integral using (9) and the fact that the integral over $\rho(\theta)$ is normalized to 1, yields

$$I_{syn}^{den} = \alpha^{fbden} g\left(\lambda^{den}(I_{syn}^{den} + C/N) + (1-\lambda^{som})I_{syn}^{som} - \Theta\right) + \alpha^{ffden}\log S .$$

We can directly solve this recurrence relation for $I_{syn}^{den}$ and get

$$I_{syn}^{den} = b^{fb}\left(\lambda^{den} C/N + (1-\lambda^{som})I_{syn}^{som} - \Theta\right) + b^{ff}\log S \quad (12)$$

with $b^{fb} = \dfrac{\alpha^{fbden} g}{1-\alpha^{fbden} g\lambda^{den}}$ and $b^{ff} = \dfrac{\alpha^{ffden}}{1-\alpha^{fbden} g\lambda^{den}}$.

We now substitute $I_{syn}^{som}$ and $I_{syn}^{den}$ given by Eqs 1 and 12 in the expression for the dendritic current, Eq. 3, and get

$$I_0^{den} = \beta^{ff}\log S + \beta^{fb}\left(C/N - \Theta/\lambda^{den}\right), \quad (13)$$

with $\beta^{ff} = \lambda^{som}\alpha^{ffsom} + (1-\lambda^{den})\left((1-\lambda^{som})\alpha^{ffsom} b^{fb} + b^{ff}\right)$

and $\beta^{fb} = (1-\lambda^{den})\lambda^{den} b^{fb} = (1-\lambda^{den})\dfrac{\alpha^{fbden} g\lambda^{den}}{1-\alpha^{fbden} g\lambda^{den}}$.

This expression for $I_0^{den}$ only contains the feedforward stimulus, log *S*, and the calcium population signal *C* (recall the definition of $\lambda^{som}$ and $\lambda^{den}$ below Eq. 3). Plugging (13) into (9) therefore yields a recurrence relation for *C(S)* ,

$$C(S) = \frac{Nc}{1+e^{-\left(\beta^{ff}\log S + \beta^{fb}\left(C(S)/N - \Theta/\lambda^{den}\right) - \theta_0\right)/\sigma}} . \quad (14)$$

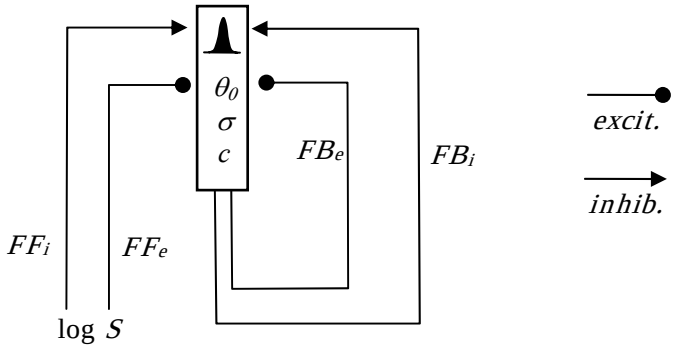


**Supplementary Figure M3.** *Analytically reduced model. The whole microcircuitry is specified by the effective strength of the feedforward ($\beta^{ff}=FF_e-FF_i$) and the feedback ($\beta^{fb}=FB_e-FB_i$) connections, each composed of an excitatory and inhibitory component. The calcium spike thresholds of the N dendrites are assumed to be Gaussian distributed around $\theta_0$ with standard deviation $\sigma$, and each calcium spike produces the signal c. The population calcium signal C as a function of the stimulus strength S is the sigmoidal function $C(S)=Nc/(1+\exp(-\gamma(\beta^{ff}\log S-(\theta_0+\theta_1))/\sigma))$ , with $\gamma=(1-\beta^{fb}c/(4\sigma))^{-1}$ and $\theta_1=-\beta^{fb}c/2$ (assuming that the action potential thresholds $\Theta$ of the pyramidal neurons are zero). We conclude that increasing the feedback connection strength $\beta^{fb}$ increases the gain $\gamma$, while increasing the feedforward connetion strength $\beta^{ff}$ mainly leads to a threshold decrease $\theta_1$ (and also to a stretching the* log*S axis which, for large $\theta_0$, becomes negligible, however).*

**Solving the calcium recurrence relation.** The recurrent Eq. 14 has only one solution in *C(S)*, provided that $\beta^{fb}$ is not too large (and in particular if $\beta^{fb}<0$ for the case that feedback inhibition dominates feedback excitation, $\alpha^{fbden}=\alpha_{ex}^{fbden}-\alpha_{inh}^{fbden}<0$ ). Tracing this unique solution for varying *S* yields a sigmoidal-like function of log *S*. To study the parameter dependency of this function we approximate it by a pure sigmoidal (i.e. a Boltzmann function) and make the ansatz

$$C(S)\approx\frac{Nc}{1+e^{-\gamma(\beta^{ff}\log S-(\theta_0+\theta_1))/\sigma}} \qquad (15)$$

with some additional gain factor $\gamma$ and some additional shift $\theta_1$. After some reasoning (see Endnote 3) one finds for the two additional parameters

$$\gamma=\frac{1}{1-\beta^{fb}c/(4\sigma)} \quad \text{and} \quad \theta_1=\beta^{fb}\left(\Theta/\lambda^{den}-c/2\right), \qquad (16)$$

with $\beta^{fb}$ defined in (13) and $\lambda^{den}$ defined in (3). Recall that the parameters $\theta$ and $\sigma$ are characterizing the calcium threshold density (8), while *c* is the strength of the dendritic calcium signal and $\Theta$ is the threshold for the somatic action potential.

Increasing the feedback strength $\alpha^{fbden}$ increases the gain of the calcium response function (because $\beta^{fb}$ in the expression of $\gamma$ is increased) and shifts the midpoint to the left (because increasing $\beta^{fb}$ makes $\theta_1$ more negative, provided that the calcium signal, after its propagation to the soma, exceeds twice the action potential threshold, $c\lambda^{den}/2>\Theta$), see Suppl. Fig. M5. Interestingly, the feedback strength $\alpha^{fbden}$ can itself be positive and the population activity is still finite, provided that the additional slope factor $\gamma$ remains itself finite. This is the case for $\beta^{fb}<4\sigma/c$.

## *The analytically reduced model*

The mathematical analysis reduced the microcircuitry with the 2-compartmental pyramidal neurons (Suppl. Fig. M1, 2) to a simple feedback circuitry for the population calcium signal *C(S)* (Suppl. Fig.

M3). According the Eq. 14 this feedback circuitry is characterized by the effective feedforward and feedback connection strengths, $\beta^{ff}=FF_e+FF_i$ and $\beta^{fb}=FB_e+FB_i$ , the number of pyramidal neurons ($N$), the strength of a unit calcium spike ($c$), the distribution of the calcium spike thresholds ($\theta_0$, $\sigma$), and the effective action potential threshold normalized by the dendritic leak factor ($\tilde{\Theta}\lambda^{den}$). This feedback circuitry for $C(S)$ can be approximated by the Boltzmann function (Eq. 15) with parameter values given in Eq. 16 (cf. Supp. Fig. M5).

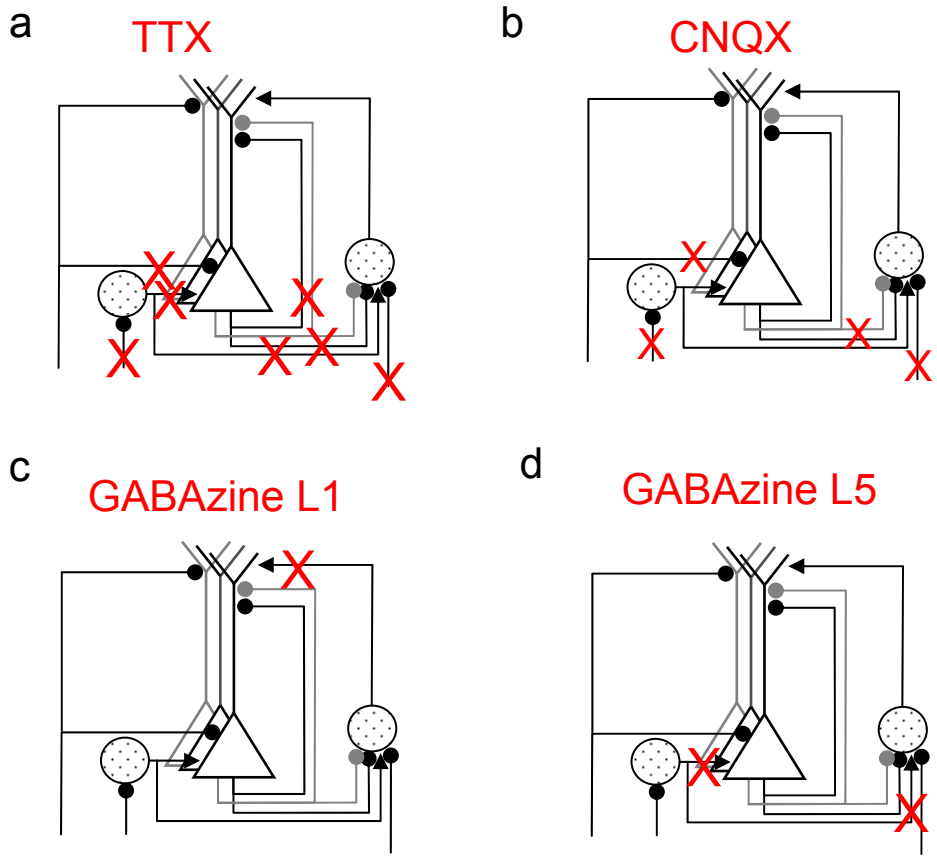


**Supplementary Figure M4.** *Modeling the blocking experiments, red crosses indicate total block, green crosses indicate partial block.* ***a****, Blocking of action potentials in L5 by local, deep layer application of TTX,* ***b*** *competitive partial blocking of excitatory AMPA receptors in L5 by deep layer application of CNQX,* ***c****, blocking of $GABA_A$ receptors in L1 by surface application of GABAzine, and* ***d****, blocking of $GABA_A$ receptors in L5 by deep layer application of GABAzine. The crossed synaptic connection strengths are set to 0 in the model. Based on the analytical reduction, the canceling of these specific connections translate into corresponding modifications of the parameters $FF_{e/i}$ and $FB_{e/i}$ characterizing the overall feedforward and feedback connection strengths (see Figs. M1, M3 and Table 1, 2).*

## *Simulation results*

The differential effects of pharmacologically modulating the feedforward and feedback connection strengths is revealed by varying the parameters $\alpha^{ffden}$ and $\alpha^{fbden}$, respectively. The main message is that reducing the strength of the feedforward connection mostly shifts the *f-I* curve to the right, while reducing the strength of the feedback connection reduces the gain (Supp. Fig. M5). The dominant shift in changing the feedforward connection is a consequence of the high threshold value $\theta_0$ for eliciting a

calcium spike. Although the feedforward connection strength multiplicatively scales the log *S* axis, the main effect is a shift due to the high threshold (Supp. Fig. M6). It is important to note that this shift arises from the model (while also present in the data) because we matched the calcium spike threshold $\theta_0$ to a physiological value ($\theta_0$ =500 pA, see Larkum et al, 2004). It would also be possible to reproduce the gain modulation by changing the feedforward strength, but at the price of setting the threshold unphysiologically to zero and not being able to reproduce the shift observed with L5 GABAzine application (see below).

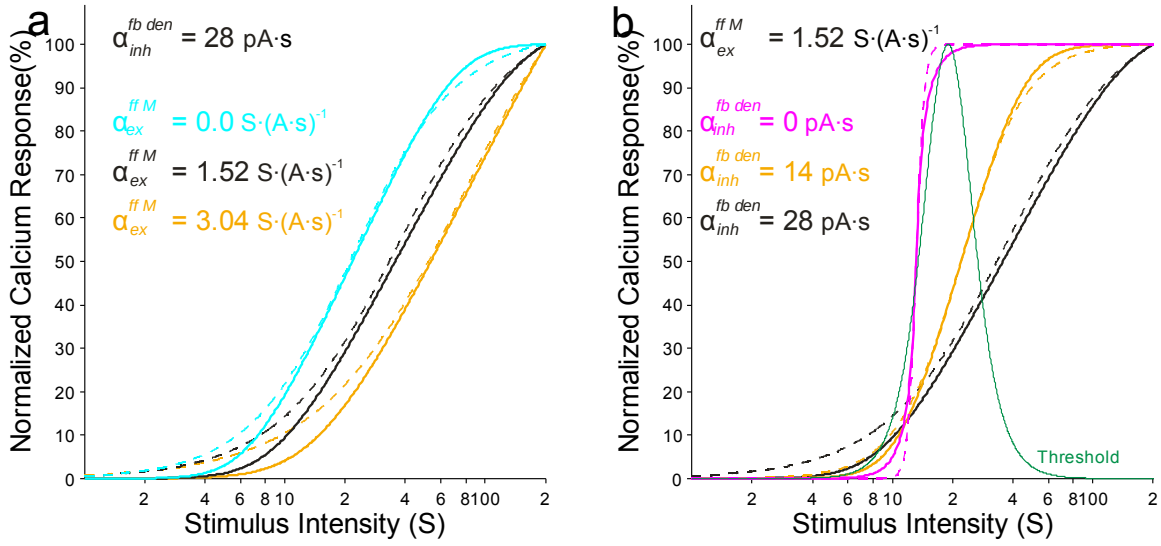


**Supplementary Figure M5.** *Effects of varying the feedforward and feedback connection strengths.* ***a****, Increasing the feedforward strength by decreasing the feedforward excitation on the Martinotti cell* $\alpha_{ex}^{ffM}$ *leads to mainly a left shift. Solid lines show the solution of the recurrent Eq. 14, and dashed lines the fits using Eq. 15 (values of* $\alpha_{ex}^{ffM}$ *from left to right: 3.04, 1.52, 0 S·(A·s)*$^{-1}$*).* ***b****, Increasing the inhibitory feedback strength* $\alpha_{inh}^{fbden}$ *(describing the inhibitory connection strengths from the Martinotti cells to the pyramidal cell dendrites) leads to an effective gain decrease* $\gamma$ *and a simultaneous right shift by* $\theta_1$ *(see Eq. 16 and the definitions in Eqs 12 and 13 ). Solid lines: solutions of Eq. 14, dashed lines: approximations by Eq. 15 (values of* $\alpha_{inh}^{fbden}$ *from left to right: 28, 14, 0 pA·s). The bell-shaped curve represents the threshold density* $\rho_\theta$ *with* $\theta$*=(log S)/*$\beta^{ff}$ *and* $\beta^{ff}$*=1.7·10*$^{-7}$*. The black curves in a) and b) correspond to the control conditions in Fig. 4d of the main text. Similarly, the blue and pink curves in a) and b) correspond to curves labeled by "No FF*$_i$*" and "No FB*$_i$*" in Fig. 4d.*

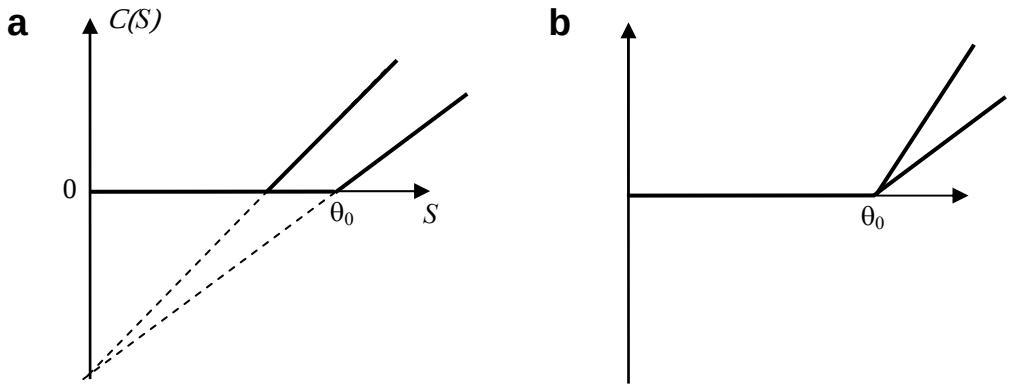


**Supplementary Figure M6.** *Differential effect of changing the feedforward and feedback connection strength.* ***a****, An increase in the feedforward connection strength* $\beta^{ff}$ *is equivalent to a scaling of the* log*S axis (see Eq. 15). In the presence of a positive threshold* $\theta_0$ *this also reduces the effective activation threshold. For the measured values of the calcium spike threshold* $\theta_0$ *the apparent change consists in mainly a threshold shift.* ***b****, An increase in the feedback connection strength* $\beta^{fb}$ *induces a pure gain modulation. The threshold is not affected because the feedback is only manifested when there is already some calcium signal, while it is absent if the calcium threshold is not exceeded.*

**Explanation of the blocking experiments.**

We modeled the local blocking of (1) AMPA receptors in layer 5 by CNQX, (2) action potentials in layer 5 by TTX, and $GABA_A$ receptors by GABAzine (3) in upper cortical layers L1 and (4) in the deep layer L5. The first three blocking experiments (CNQX, TTX, GABAzine in L1) are assumed to disinhibit dendritic calcium receptors in layer 5 pyramidal cells, and thus increase the maximum calcium response given by the product $Nc$. They are also assumed to weaken the effective feedback strength by shifting $\beta^{fb}$ towards positive values, while the effective feedforward strength $\beta^{ff}$ remains roughly unchanged (see Suppl. Figs. M4, M7 and Table 1, 2). Since the calcium spike mechanism can be blocked by specific inhibition in an all-or-none fashion, we assumed that the unit calcium event $c$ remained unchanged while the number of available pyramidal neurons $N$ in which dendritic calcium spikes can be triggered is changed. Hence, the three parameters which were used to fit the four blocking experiments were $\beta^{ff}$, $\beta^{fb}$, and $N$ (see Table 1 and 2 and Fig. M7). Note that among these 3 parameters, only 2 were considerably changed ($\beta^{fb}$ and $N$) while the third ($\beta^{ff}$) remained roughly constant.

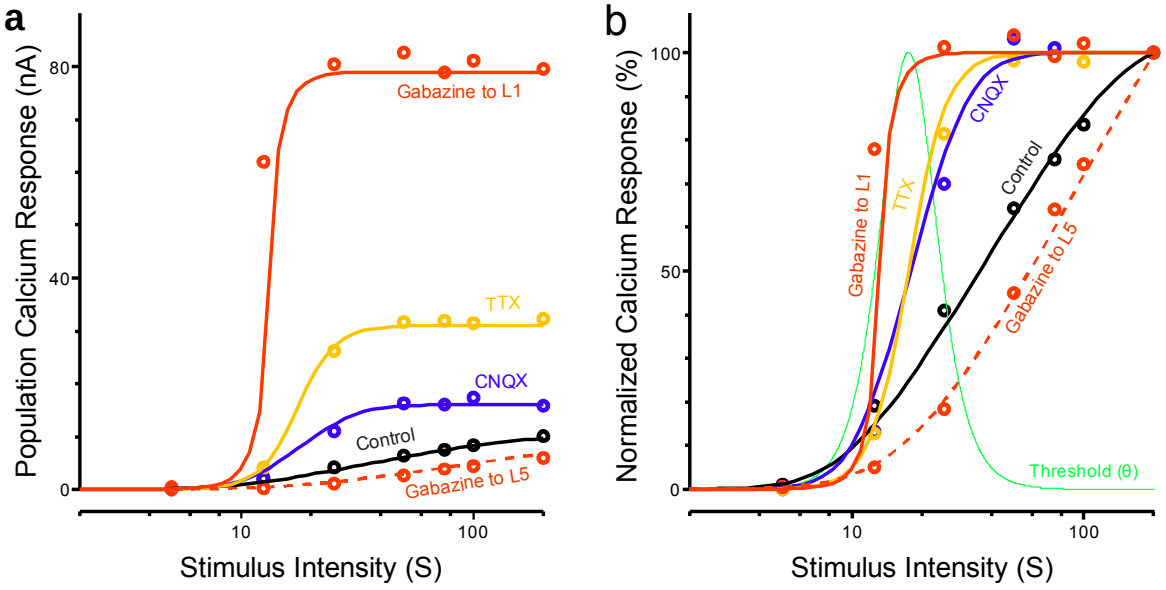


**Supplementary Figure M7:** *Modeling the effects of CNQX, TTX and Gabazine to L1 and L5 according to the scheme in Fig. M4.* ***a****, Calcium response function C(S) obtained from solving Eq. 14 and using the parameter values given in Table 1.* ***b****, Normalized data from a). Note that Gabazine to L5 does not change the gain, consistent with the interpretation that in L5 it only affects feedforward projections. All other blocking experiments, in contrast, increase the overall feedback connections and thus lead to a gain increase compared to control. The bell-shaped curve is showing the density* $\rho\theta$ *with* $\theta=(\log S)/\beta^{ff}$ *and* $\beta^{ff}=1.7\cdot10^{-7}$.

**Detailed fitting procedure**

The values for the parameters $c$ , $\theta_0$ , $R_m^{som}$ , $R_m^{den}$ , $R_T$ , $\Theta$, and $g$ arising in Table 1 are extracted from the data published in Larkum et al. (2004). From these we calculated the dendritic leak factors $\lambda^{den}$ and $\lambda^{som}$ (see Table 2). To obtain the fits in Fig. M7 we first considered the TTX experiment where all connections except the excitatory feedforward inputs to the dendrites ($\alpha^{ffden}$) are put to 0 (cf. Fig. M4). In this case the calcium signal takes the form $C(S) = Nc/(1+\exp(-(\beta^{ff} \log S - \theta_0)/\sigma)$ with $\beta^{ff}=(1-\lambda^{den})\alpha^{ffden}$ (see Eqs 15 and 12, 13). By fitting this function to the data we extracted the TTX-specific values for $\alpha^{ffden}$ and $N$. We also extracted the value of σ characterizing the width of the calcium threshold distribution which was then fixed also for the other four response curves.

The data of the remaining experiments (control, CNQX, GABAzine in L1, GABAzine in L5) were fitted by optimizing the parameters $\beta^{ff}$, $\beta^{fb}$, and $N$ appearing in Eq. 14 for each experiment separately. From the effective connection strengths $\beta^{ff}$ and $\beta^{fb}$ we calculated the physiological connection strengths $\alpha^{ffden}$ , $\alpha^{ffsom}$ and $\alpha^{fbden}$ by using the formulas following Eqs 12 and 13. Assuming the blocking patterns specified by the factors in Table 1 one can now uniquely decompose $\alpha^{ffden}$ , $\alpha^{ffsom}$ and $\alpha^{fbden}$ into the components specified in Table 1 (see also the formulas in Table 2).

| **Parameters of the full model** | **Units** | **Control (value)** | **CNQX (factor)** | **TTX (factor)** | **Gabazine (factors)** L1 | L5 |
|---|---|---|---|---|---|---|
| $N$ (number of pyramidal dendrites generating the population signal) | no un. | 10 | 1.6 | 3.1 | 7.9 | 1 |
| $\alpha_{ex}^{fbden}$ (excitat. dendritic feedback strength) | pA·s | 6 | 1 | 0 | 1 | 1 |
| $\alpha_{inh}^{fbden}$ (inhibit. dendritic feedback strength) | pA·s | 28 | 0.4 | 0 | 0 | 1 |
| $\alpha_{ex}^{ffM}$ (exc. feedforw. str. to Martinotti cell) | $S\cdot(A\cdot s)^{-1}$ | 1.52 | 0.4 | 0 | 1 | 1 |

| | | | | | | |
|---|---|---|---|---|---|---|
| $\alpha_{inh}^{ffM}$ (inhib. feedforw. str. to Martinotti cell) | S·(A·s)$^{-1}$ | 1.75 | 1 | 0 | 1 | 0 |
| $\alpha_{ex}^{ffsom}$ (excit. somatic feedforward strength) | pS | 20 | 0.4 | 0 | 1 | 1 |
| $\alpha_{inh}^{ffsom}$ (inhib. somatic feedforward strength) | pS | 10 | 0.4 | 0 | 1 | 0 |
| $\alpha_{ex}^{ffden}$ (excitat. dendritic feedforw. strength) | pS | 240 | | | | |
| $c$ (unit dendritc calcium signal) | pA | 100 | | | | |
| $\theta_0$ (mean calcium threshold) | pA | 500 | | | | |
| $\sigma$ (half-width of $\theta$-distribution) | pA | 33 | | | | |
| $R_m^{som}$ (som. membrane resist.) | MΩ | 50 | | | | |
| $R_m^{den}$ (dendr. membr. resistance) | MΩ | 43 | | | | |
| $R_T$ (transfer resistance) | MΩ | 65 | | | | |
| $\Theta$ (action potential threshold) | pA | 200 | | | | |
| $g$ (gain of *f-I* transfer function) | (pA·s)$^{-1}$ | 0.07 | | | | |

**Table 1:** *Parameters of the full model used in Suppl. Fig. M7 and their physiological interpretation. The columns "CNQX", "TTX", GABAzine L1" and "GABAzine L5" give the factors with which the control value is multiplied to mimic the pharmacological interventions as depicted in Suppl. Fig. M4. Given the pattern of blocking factors, we tuned the values of first 7 parameters in the control column to fit the 5 response functions (each characterized by 3 parameters). The remaining parameters (except $\sigma$) were extracted from Larkum et al. (2004). Note that N is a nonlinearly increasing function of the feedback connection strength $\alpha^{fbden}$ and roughly a linearly increasing function of the gain factor $\gamma$ (see Table 2).*

| **Parameters of the analytically reduced model** | **Units** | **Control** | **CNQX** | **TTX** | **Gabazine** | |
|---|---|---|---|---|---|---|
| | | | | | **L1** | **L5** |
| $\alpha^{fbden}$ (feedback strength to den) | pA·s | -22.0 | -5.2 | 0.0 | 6.0 | -22.0 |
| $\alpha^{fbden} = \alpha_{ex}^{fbden} - \alpha_{inh}^{fbden}$ | | | | | | |
| $\alpha^{ffden}$ (feedforward strength to den) | pA·s | 246.4 | 252.8 | 240.0 | 240.0 | 197.4 |
| $\alpha^{ffden} = \alpha_{ex}^{ffden} - \alpha_{inh}^{fbden}\left(\alpha_{ex}^{ffM} - \alpha_{inh}^{ffM}\right)$ | | | | | | |
| $\alpha^{ffsom}$ (feedforw. strength to soma) | pA·s | 10 | 0.8 | 0 | 0.1 | 0.2 |
| $\alpha^{ffsom} = \alpha_{ex}^{ffsom} - \alpha_{inh}^{ffsom}$ | | | | | | |
| $\beta^{ff}$ (effect. feedforw. str. to dendrite) | pA·s | 124.2 | 168.6 | 147.7 | 202.8 | 96.8 |
| $\beta^{fb}$ (effect. feedback str. to dendrite) | no un. | -215.0 | -65.5 | 0.0 | 93.3 | -215.0 |
| $\lambda^{den}$ (dendritic leak factor) | no un. | 0.2722 | | | | |
| $\lambda^{som}$ (somatic leak factor) | no un. | 0.3165 | | | | |
| $\gamma$ (gain factor of response function) | no un. | 0.38 | 0.67 | 1.0 | 3.47 | 0.38 |
| $\theta_1$(additional shift of calcium thresh.) | pA | -50.49 | -15.41 | 0 | 22.06 | -50.49 |

**Table 2:** *Derived parameters of the model, calculated from the values in Table 1. The parameters $\alpha$ give the compound connection strengths, while $\beta^{ff}$ and $\beta^{fb}$ yield the effective feedforward and feedback connection strengths, $\beta^{ff}=FF_e-FF_i$ and $\beta^{fb}=FB_e-FB_i$, in the reduced model (Eqs 14 – 16 and Suppl. Fig. M3, calculated from the formulas following Eqs 12 and 13). The dendritic and somatic leak factors $\lambda^{den}$ and $\lambda^{som}$ are calculated from the passive neuronal parameters according to the formulas following Eq. 3. For the definition of $\gamma$ and $\theta_1$ see Eq. 16.*

**Bibliography**
Larkum M, Senn, W and Lüscher H-R (2004), "Top-down dendritic input increases the gain of layer 5 pyramidal neurons.", *Cerebral Cortex*, 14:1059-1070

Pérez-Garci E, Gassmann M, Bettler B, Larkum ME. (2006), "The GABAB1b isoform mediates long-lasting inhibition of dendritic $Ca^{2+}$ spikes in layer 5 somatosensory pyramidal neurons." *Neuron*. 18;50(4):603-16.

---

[i] **Somato-dendritic voltage interactions.** The total dendritic and somatic steady state currents are obtained from solving the coupled differential equations governing the somatic and dendritic voltages,

$$C\,dV^{som}/dt = -V^{som}/R_m^{som} + I_{syn}^{som}(S) + (V^{som} - V^{den})/R_T$$

$$C\,dV^{den}/dt = -V^{den}/R_m^{den} + I_{syn}^{den}(S) + c_i(S) + (V^{den} - V^{som})/R_T \quad .$$

Setting the derivatives to 0 and abbreviating $I^{som}=V^{som}/R_m^{som}$ and $I^{den}=V^{den}/R_m^{den}$ (while suppressing the index *i*), we can solve for these quantities and get (6) as well as

$$I_i^{den}(S) = \lambda^{som} I_{syn}^{som}(S) + (1-\lambda^{den})\left(I_{syn}^{den} + c_i(S)\right) \qquad (6')$$

with $\lambda^{som}$ and $\lambda^{den}$ defined below Eq. 3. Considering Eqs (6) and (6') together we recognize Kirchhoff's law, stating here that the total membrane current is preserved in the two electrotonically coupled compartments.

[ii] **Integration of the population calcium signal.** The last expression in (9) is obtained by noticing that the derivative of the second integral with respect to $I_0^{den}$ is $Nc\rho I_0^{den}$. To calculate this derivative we use that the derivative of the step-function $\Theta$ is a $\delta$-function. But $Nc\rho I_0^{den}$, with $\rho$ defined in (8), is also the derivative of the last expression in (9) with respect to $I_0^{den}$.

[3] **Parameter identification for the population calcium response as a sigmoidal.** To calculate the additional shift $\theta_1$ of the sigmoidal approximation of *C(S)* (see Eqs 14 and 15) we note that the total shift of the function *C(S)* along the $s=\beta^{ff}\log S$ axis corresponds to the value of *s* where the function *C(S)/N* definded by Eq. 14 (after division by *N*) reaches its half maximum, i.e. *C(S)/N=c/2*. Replacing *C(S)/N* with *c/2* on the right-hand-side of Eq. 14 yields the condition $s + \beta^{fb}\left(c/2 - \Theta/\lambda^{den}\right) - \theta_0 = 0$ on *s* for *C(S)/N* reaching this half maximum. Equating this with the ansatz in (15) gives $s + \beta^{fb}\left(c/2 - \Theta/\lambda^{den}\right) - \theta_0 = s - (\theta_0 + \theta_1)$, from where we get $\theta_1 = \beta^{fb}\left(\Theta/\lambda^{den} - c/2\right)$ as defined in (16).

To calculate the additional gain factor $\gamma$ of the sigmoidal approximation of *C(S)* we first consider the derivative of *C* given in (14) with respect to $s=\beta^{ff}\log S$ at the point where *C* reaches the half maximum *Nc/2*. This derivative is calculated to be $C' = (1+\beta^{fb}C'/N)\cdot Nc/(4\sigma)$. Solving for *C'* yields $C' = \gamma\, Nc/(4\sigma)$ with additional gain factor $\gamma = (1-\beta^{fb}c/(4\sigma))^{-1}$ as defined in (15) and (16).